NANO LETTERS

pubs.acs.org/NanoLett Letter

The Strongest Size in Gradient Nanograined Metals

Penghui Cao*

Cite This: *Nano Lett.* 2020, 20, 1440−1446 Read Online

ACCESS | Metrics & More | Article Recommendations | Supporting Information

ABSTRACT: Conventional polycrystalline metals become stronger with decreasing grain size, yet softening starts to take over at the nanometer regime, giving rise to the strongest size at which the predominate strengthening mechanism switches to softening. We show that this critical size for the onset of softening can be tuned by tailoring grain size gradient, and raising in the gradient shifts the size toward the smaller value. The decrease in the strongest size is prompted by mitigation of grain boundary-mediated softening processes accompanying by enhanced intragranular plastic deformations. We found that the nanograins smaller than 6 nm, mainly involving intergranular sliding in homogeneous structures, reveal anomalous plastic deformation in gradient systems, which is mediated by partial dislocation nucleation, faulting and twinning activated in a gradient stress field. The results on extended dislocation slip and gradient plasticity, stemming from the structure heterogeneity, shed light on an emerging class of heterogeneous nanostructured materials of improved strength−ductility synergy.

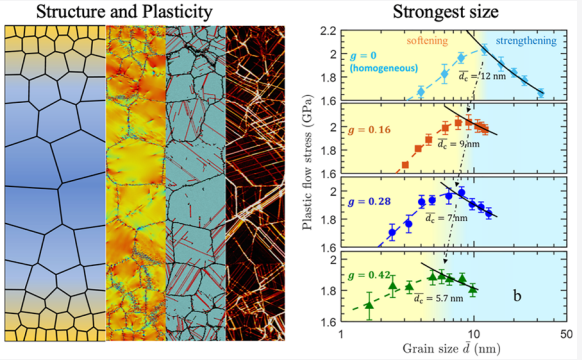

KEYWORDS: *strongest size, gradient structure, gradient plasticity, dislocations, nanocrystalline metal*

The strength and hardness of polycrystalline metals greatly increases when reducing their grain size, commonly understood as the classical Hall−Petch strengthening[1,2] due to dislocation pileup on grain boundary obstacles.[3] As grain size becomes smaller, the increase of grain boundary density enhances blocking of dislocation glide, therefore strengthening the materials.[4] However, an inverse Hall−Petch effect, a reduction in strength with decreasing grain size, arises in nanocrystalline metals with grain size of a dozen manometers.[5−7] The variation of strength with grain size suggests a characteristic size d_c, at which the predominate deformation mechanism changes from strengthening to softening, owing to grain boundary-mediated processes such as sliding and migration. In view of grain size dependent strength in noncrystalline metals, the "strongest size" d_c emerges,[8] suggesting the strengthening effects reach the maximum at this critical length. For conventional homogeneous nanograined (NG) metals, the d_c has been found to occur at grain size of about 50 to 10 nm.[4,7]

Recently, an otherwise material with nonhomogeneous or heterogeneous nanostructures[9] has drawn increasing research interests because of the unprecedented mechanical properties that unfolded[10,11] as well as the advances in processing and manufacturing routes for producing heterogeneous materials.[12] For example, a variety of gradient nanostructured metals[13,14] and alloys[15,16] with a spatial gradient in grain size achieve a noteworthy combination of high strength and high ductility. This improved strength−ductility synergy can be attributed to production and storage of geometrically necessary dislocations for compatible deformation in heterogeneous structures,[17] that brings about extra hardening during deformation and, hence, achieves higher ductility as compared with homogeneous noncrystalline systems. Because of the structural heterogeneity in gradient nanograined (GNG) metals and possibly new deformation mechanisms, it would be interesting to ask whether the aforementioned strongest size d_c varies with an imparted gradient in grain size and what associated mechanisms are responsible for a change of d_c if at all. Answering these questions is not only of fundamental interest but will also shed light on the perspective of tailoring mechanical behaviors of materials by tuning nanostructural heterogeneity.

In this study, massively parallel atomistic simulations were performed in GNG and homogeneous NG samples of Cu, a material which has been extensively studied in experiments and simulations.[5,13,18,19] The results reveal that the size d_c of GNG structures becomes smaller as compared with their homogeneous counterparts, and increasing the gradient in grain size will drive the strongest size to a smaller value. By analyzing the deformation trajectories, it is found that the softening processes of grain boundary sliding and migration in the GNG are greatly mitigated, which are accompanied by enhanced plastic deformations mediated by activating multiple dislocation slip

Received: December 18, 2019
Revised: January 15, 2020
Published: January 16, 2020

https://dx.doi.org/10.1021/acs.nanolett.9b05202
Nano Lett. 2020, 20, 1440−1446

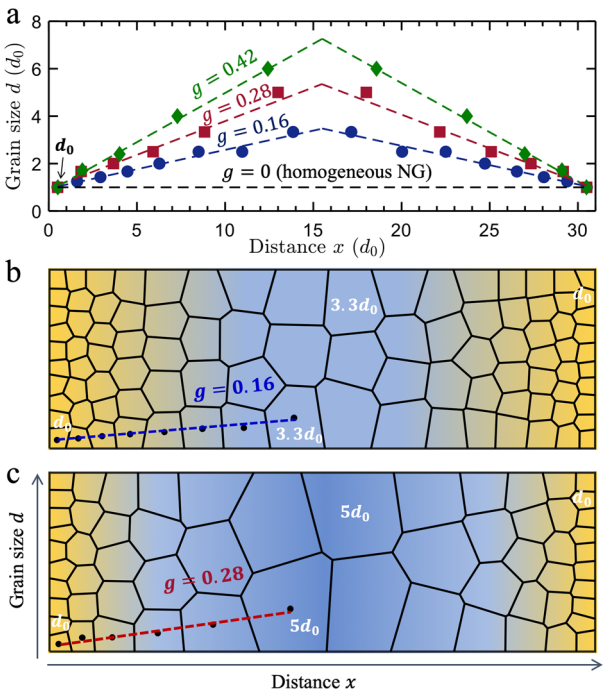

Figure 1. (a) Variation of grain size with respect to distance from the boundary. Four systems with different grain size gradients are considered, and it is noted the zero-gradient g = 0 represents the homogeneous nanocrystalline system. (b, c) Spatial distribution of grains for g = 0.16 and 0.28, respectively. The d_0 describes the smallest grain in a GNG structure.

systems, deformation nanotwins, and stacking faults. The boundary stabilization and enhanced plasticity resulting from the grain size gradient suggest the fundamental deformation mechanisms underlying extraordinary work hardening and high ductility of many heterogeneous structured metals.

Four systems with different gradients are considered, and Figure 1a shows their grain size variation with distance x from the boundary. The spatial gradients in grain size g, defined as the first order derivative of grain size d with respect to x, are 0, 0.16, 0.28, and 0.42 for the studied systems. The zero gradient g = 0 represents homogeneous nanograined structures, and d_0 represents the smallest grain size in a GNG structure. The GNG and homogeneous NG samples are created as randomly orientated grains produced by Voronoi tessellation.[20] To construct different sized GNG structures of the same gradient, the crystallographic grain orientations and gradient are kept constant when scaling the structure to different sizes. We created 34 samples for the four sets of gradients with the smallest one containing 1.05×10^5 atoms and the largest one having 7.5×10^7 atoms (see section 1 in the Supporting Information for sample details). Figure 1b and c depicts the spatial distributions of grains for g = 0.16 and 0.28, respectively. The interatomic interaction of Cu atoms was modeled with an embedded-atom method potential,[21] and all simulations were performed at a constant temperature of 300 K using Nosé–Hoover thermostat.[22,23] Periodic boundary conditions are imposed in all three directions, and uniaxial tensile strain is applied to the sample in the direction perpendicular to the gradient (i.e., y axis shown in Figure 1c). The stress is calculated by considering the components of kinetic energy tensor and the virial tensor from pairwise interaction. All samples are deformed at a constant

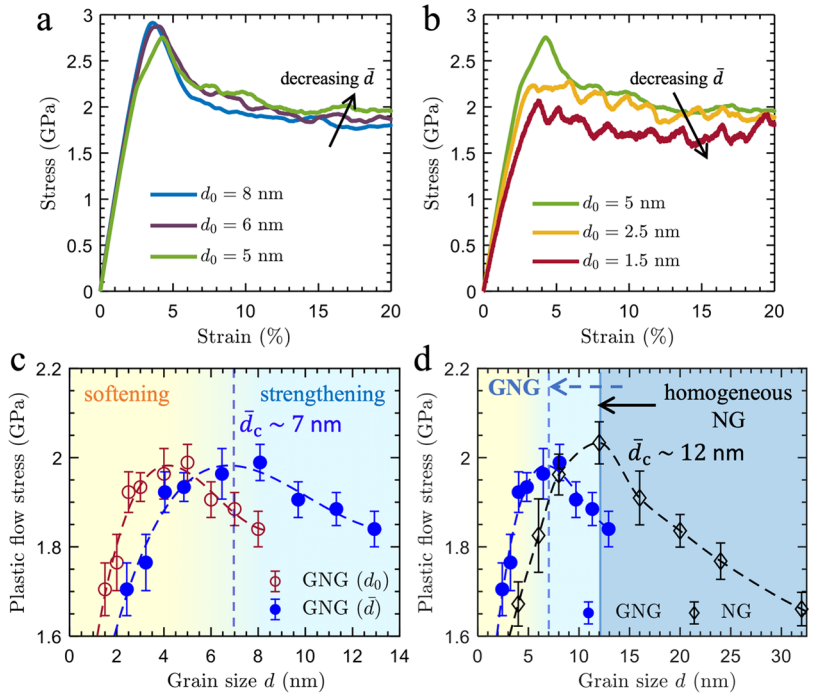

Figure 2. Stress–strain behaviors of GNG Cu with g = 0.28 and the strongest size. (a, b) Tensile stress–strain curves for different sized GNG samples, labeled by its smallest grain d_0. (c) Variation of plastic flow stress as a function of mean grain size $\bar{d}$ (filled blue circles) for GNG. The flow stress as a function of d_0 (red circles) is also plotted for comparison. The critical size $\bar{d}_c$ = 7 nm, separating the strengthening and softening regimes, is approximated by fitting the date to polynomial functions. (d) For comparison, the stress variation with grain size for homogeneous NG samples is included, exhibiting the critical grain size of d_c = 12 nm. The plastic flow stress is calculated as the average stress from the strain interval of 10–20% . Error bars characterize the standard deviation of fluctuation in the strain interval.

https://dx.doi.org/10.1021/acs.nanolett.9b05202
Nano Lett. 2020, 20, 1440–1446

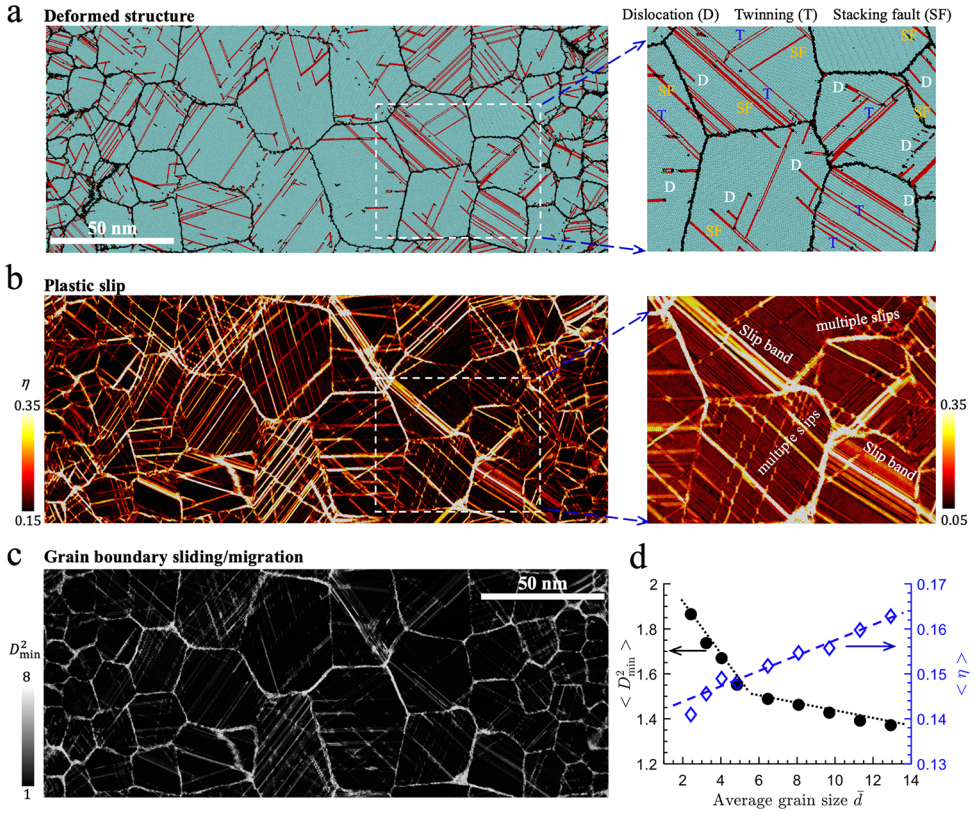

Figure 3. Deformation mechanisms in the GNG Cu with g = 0.28 and d_0 = 8 nm. (a) Deformed atomic structure at 15% strain shows multiple deformation modes appearing in the system, involving dislocations, nanotwins, and stacking faults. (b) Spatial distribution of shear strain η. Both small and large grains exhibit intragranular plastic slips, and the intersection of slips suggests that multiple slip systems are activated. (c) Spatial distribution of nonaffine displacement D_{min}^2. The small grains appear to show no apparent increase in nonaffine displacement, implying gradient-mediated grain boundary stabilization. (d) Nonaffine displacement D_{min}^2 and shear strain $\langle\eta\rangle$ as a function of $\bar{d}$ for the 9 different sized GNG samples.

strain rate of 5×10^8 s^{-1}, and the stress in other directions perpendicular to tensile deformation is controlled at zero stress using Berendsen barostat.[24]

The responses of system-level stress to uniaxial strain for GNG structures are shown in Figure 2a and b, in which the curves are labeled by its smallest grain d_0, ranging from 8 to 1.5 nm. It can be seen that the overall stress−strain response consists of an initially elastic loading up to a yield point, followed by a steady state plastic flow after about 10% tensile strain. When comparing these curves, Figure 2a shows the flow stress shifts upward with decreasing grain size. However, the relationship between flow stress and grain size becomes opposite with a further decrease of grain size (Figure 2b). The dependence of plastic flow stress on grain size is shown in Figure 2c, revealing that the flow stress increases with decreasing grain size, attaining the maximum at the critical value $\bar{d}_c \sim 7$ nm. After that, the softening takes over from the strengthening and the stress decreases sharply with further decreasing $\bar{d}$. Here, the $\bar{d}$ represents the averaged grain size, determined as the mean value of all grain sizes in a system (see Figure S3 for the statistical distribution of grain size). The dependence of flow on grain size for a homogeneous NG structure is included in Figure 2d, which exhibits a critical value of 12 nm, consistent with previous investigations.[4,5] It is evident that, by introducing the grain size gradient, the threshold size shifts from 12 nm to a smaller value of 7 nm, suggesting the strengthening mechanisms continue to predominate and extend to systems with smaller grains (see Figure S5 for gradient g = 0.16 in the Supporting Information).

To elucidate deformation mechanisms, we show a typical deformed atomic structure of a GNG sample at 15% applied strain in Figure 3a. One can see dislocations, stacking faults, and nanotwins appear, suggesting that multiple plastic deformation processes have been triggered during deformation even in small nanograined domain. This structural characterization, which is analyzed on the immediate strained configuration, clearly reveals the ongoing elementary processes underlying plastic deformation. However, it is impossible to track and unveil the deformation history that the system has experienced, because, for example, no footprint (defect) will be left over in a grain after a full dislocation glides through it. To reveal the history of plastic deformation and grain boundary processes, we calculate the atomic-level deformation by breaking it down into affine plastic deformation and nonaffine rearrangement[25,26,27] according to

$$\mathbf{d}_{ij} = \mathbf{J}_i \mathbf{d}_{ij}^0 + \delta\mathbf{d}_{ij} \tag{1}$$

where $\mathbf{d}_{ij}$ is distance vector between atom i and j in the current state and $\mathbf{d}_{ij}^0$ is for the initial undeformed state. The deformation tensor $\mathbf{J}_i$ reflects local affine deformation like slip, and $\delta\mathbf{d}_{ij}$ measures nonaffine atomic rearrangements. The $\mathbf{J}_i$ for the atom i is calculated by minimizing

$$D_i^2 = \sum_{j=1}^{n_i} |\mathbf{d}_{ij} - \mathbf{J}_i \mathbf{d}_{ij}^0|^2 \tag{2}$$

where n_i is total neigbors around atom i. From $\mathbf{J}$, the Green strain tensor and its invariant, shear strain η, can be calculated that is a good measure of local inelastic deformation. The minimized D_i^2

https://dx.doi.org/10.1021/acs.nanolett.9b05202
Nano Lett. 2020, 20, 1440−1446

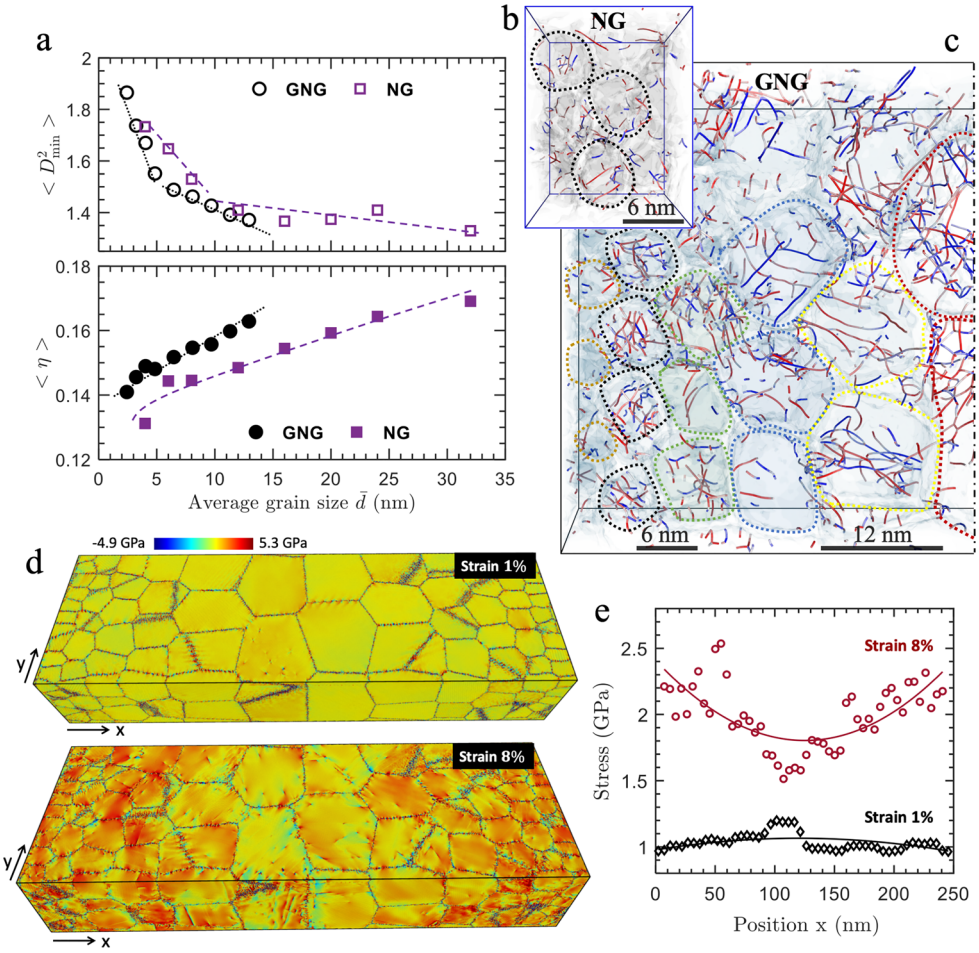

Figure 4. Comparison of deformation mechanisms in GNG and homogeneous NG samples, and stress distributions. (a) Variation of D_{min}^2 and $\langle\eta\rangle$ as a function of grain size $\bar{d}$. (b, c) Dislocation distributions in homogeneous NG (b) and GNG samples (c) at the same strain of 20%. GNG shows intensified dislocations even in 6 nm sized grain. Red lines represent screw dislocations, and blue lines show edge dislocations. (d) Distributions of atomic tensile stress at two applied strains of 1% and 8%. The corresponding tensile stress variation with position for the two strained states are shown in (e).

measures the nonaffine squared atomic rearrangement which is not captured by **J**. The processes such as dislocation slip, twinning, and formation of stacking fault, involving an ordered transformation, are major contributions to the affine deformation. The activities of amorphous-like GBs, including migration and sliding, predominately contribute to the nonaffine deformation. For example, the sliding of GB, which is analogous to shear-band sliding in amorphous solids,[28] involves shear transformation-like events that increase the nonaffine displacement.

Figure 3b shows the spatial distribution of atomic shear strain η of the system at the same strained state as in Figure 3a. The appearance of abundant bright lines of large strain implies that dislocations have passed through the grains for multiple times. The large plastic slip primarily occurs in the grain interiors, where the intersections of slips indicate that multiple slip systems have been activated during deformation. In Figure 3c, we show the nonaffine squared displacement D_i^2 corresponding to the same state of Figure 3b. The large nonaffine rearrangements mainly take place in the grain boundaries, confirming D_i^2 as an appropriate measure for grain boundary activities including sliding and migration. It is noted that the boundary-related process in the areas of small nanograins exhibit no apparent increase as compared with that of large grains (see Figure 3c), suggesting a gradient architecture-inducing grain boundary stabilization. These boundary-related processes, softening the strength of the materials, can be caused by different mechanisms such as stress-induced intergranular sliding,[29] dislocation-grain boundary interaction,[30] and shear-coupled boundary migration.[31,32] It is interesting to note that substantial grain growth caused by stress-induced grain boundary migration has been clearly revealed in experiments,[13] which is responsible for the plastic deformation of GNG materials. To explicitly extract grain boundary migration from boundary activities, we compare the grain boundary networks between undeformed and strained states (see Figure S4 in the Supporting Information), and during plastic deformation the grain boundaries experience apparent migration, resulting in growth of grains at the expense of their neighbors.

To understand how the grain size $\bar{d}$ affects plastic slip and grain boundary process in GNG systems, we survey the shear strain $\langle\eta\rangle$ and the nonaffine squared displacement $\langle D_{min}^2\rangle$ and plot them as a function of $\bar{d}$ in Figure 3d, where each data point represents a GNG system. The system-averaged $\langle\eta\rangle$ decreases with decreasing grain size $\bar{d}$ in a virtually linear manner, except for the smallest GNG sample of $\bar{d}$ = 2.4 nm, because it only contains fine grains which are smaller than ~12 nm; therefore, the system is losing dislocation-mediated plastic deformability.

https://dx.doi.org/10.1021/acs.nanolett.9b05202
Nano Lett. 2020, 20, 1440−1446

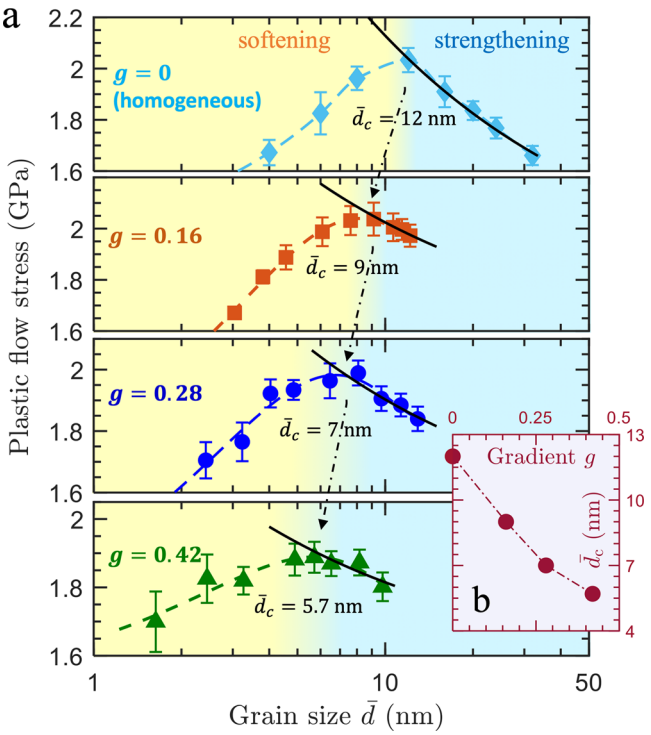

Figure 5. Dependence of critical grain size $\bar{d}_c$ on structure gradient g. (a) Variation of flow stress with mean grain size $\bar{d}$ for structures with gradients g = 0, 0.16, 0.28, and 0.42. The black solid lines are fitted Hall-Petch equations. (b) The strongest size $\bar{d}_c$ decreases with increasing gradient g.

This $\langle\eta\rangle$–$\bar{d}$ behavior indicates that the extent of plastic deformations is lowered by reducing the grain size, which may be ascribed to the limited dislocation nucleation and motion which are severely confined by small regions. In contrast to the plastic slip, the nonaffine rearrangement $\langle D_{min}^2\rangle$ shows an increase with decreasing $\bar{d}$, but revealing a clear bimodal pattern. This transition behavior of $\langle D_{min}^2\rangle$, occurring at a characteristic size ~7 nm, concurs with the flow stress variation with grain size (see Figure 2c). Therefore, we regard the results to suggest the strength softening with decreasing grain size is essentially dictated by the increased boundary-mediated processes rather than the reduction of intragranular plasticity.

Figure 4a compares the deformation behaviors between GNG and homogeneous NG by showing $\langle D_{min}^2\rangle$ and $\langle\eta\rangle$ as a function of grain size. It is shown that the value of $\langle D_{min}^2\rangle$ in GNG is smaller than that of the homogeneous structure. The lowered $\langle D_{min}^2\rangle$ signifies that the boundary sliding and migration are mitigated in GNG systems, implying the grain boundary is stabilized by the imparted gradient. On the other hand, the plastic deformation is intensified in GNG systems as shown by the $\langle\eta\rangle$. It is reasonable to conclude that the grains in the GNG undergo larger plastic strain than those of homogeneous NG and hence attain extra plastic deformability. The augmented intragranular plastic deformation in GNG systems can be attributed to the formation of deformation nanotwins and stacking faults (Figure 3a) and especially to the activation of extended partial dislocations, which are activated in the gradient stress field (see discussion of Figure 4d). Figure 4b and c shows the spatial distribution of dislocation in homogeneous NG and GNG structures, respectively. The ~6 nm sized grains in NG show few dislocations, as the deformation is predominated by boundary sliding. In contrast, the GNG exhibits abounded partial dislocations even in these ultrafine grains. This means the partial dislocation slip, which is suppressed in homogeneous nanograins, becomes activated in the gradient systems.

The extended dislocation slip and enhanced plasticity root from the introduced structure gradient. When a homogeneous NG material is under a uniform tension strain, the onset of plasticity takes place in grains ideally spanning the whole system, leading to a uniform stress distribution. For a GNG system, the stress uniformity is broken down, even at the elastic deformation stage (Figure 4d). Because the small grained region consists of a higher density of grain boundary than that of the coarse-grained part, the elastic stress shows a slight decrease from the coarse grain to fine grain regions, exhibiting a convex-like profile (black curve in Figure 4e). This stress gradient is becoming reversed in the onset of plastic deformation, due to grain size dependent yielding strength (bottom panel of Figure 4d). Entering into the plastic deformation regime, the coarse grains will first undergo plastic deformation and release the internal stress, progressively changing the stress distribution to concave-like (red curve in Figure 4e). With increasing the applied strain, the plastic processes spread gradually to finer grains, triggering dislocation processes even in small grains, which is attributed to the extended dislocation slip.

To address an interesting question of how the strongest size depends on the structure gradient, we show in Figure 5a the variations of flow stress with grain size $\bar{d}$ for g = 0, 0.16, 0.28, and 0.42, as labeled. It can be seen the critical $\bar{d}_c$ shows a decrease with increasing gradient g (Figure 5b), suggesting $\bar{d}_c$ shifts to a smaller value when increasing the structure gradient. In Figure 5a, the data points in the strengthening regimes are fitted to the Hall–Petch formula $\sigma_{flow} = \sigma_0 + k_{GB}/\sqrt{\bar{d}}$, obtaining strengthening coefficient k_{GB} = 3276, 1642, 1505, and 885 MPa for gradients of 0, 0.16, 0.28, and 0.42, respectively. The decrease of k_{GB} implies the pure grain boundary strengthening becomes weakened, due to the increased volume fraction of large grains with growing in gradient. It is worth noting that the strain rate in MD simulations is several orders of magnitude higher than that of conventional laboratory experiments. With sufficiently decreasing strain rate, thermally activated diffusional processes, such as vacancy-mediated dislocation climb and creep, can occur and lower the yielding and plastic flow stresses of a system. Because vacancy diffusion along grain boundaries is much faster than bulk lattice diffusion, the small-grained materials with abundant boundaries are more susceptible to the strain rate. It is reasonable to speculate that, if diffusional plasticity and creep become as competing processes, the strongest size may drift to a larger value.

Experimental results have shown the enhanced ductility for GNG metals when comparing with their homogeneous counterparts. The improved ductility can stem from the grain size gradient, which produces gradient stress and deformation fields and promotes nucleation and storage of extended dislocations. The plasticity gradients, which gradually release the stress from large grains to small grains with increasing applied strain, mitigate strain localization and prevent early necking, hence improving ductility. For concerted deformation between adjacent small and large grains, geometrically necessary dislocations must be stored, which provides an extra strengthening mechanism, postponing the necking instability.

The study reveals the onset of strength softening in gradient nanograined Cu shifts to markedly small grains as compared with its homogeneous counterpart. It is found that the decrease

https://dx.doi.org/10.1021/acs.nanolett.9b05202
Nano Lett. 2020, 20, 1440–1446

of the strongest size results from the synergistic effect of mitigation of grain boundary sliding/migration and enhanced intergranular plastic deformation. Grain boundary-mediated softening processes, such as sliding,[18,33] grain rotation,[34,35] and migration,[29] have emerged as the prominent deformation mode for homogeneous nanocrystalline metals. When the boundary sliding takes over from the mechanism of dislocation nucleation and motion-controlled deformation, strain localization and eventually nanoracks would develop in the adjacent nanograins due to the limited dislocation slips and unconcerted deformation. In contrast to grain boundary stabilization through segregation engineering,[36,37] the results suggest that grain boundary resistance to sliding and migration can be tuned by tailoring its spatial distribution. As a result of the boundary stabilization, the intragranular plastic deformation, involving processes of partial dislocation, stacking faults, and nanotwins, is triggered and prompted to accommodate the applied mechanical strain. The activation of partial dislocations, especially in small grains, enables system stalling and storing of geometrically necessary dislocations which are required for compatible deformation of heterogeneous materials. The storage of geometrically necessary dislocations, in the vicinity of the grain boundary[17] or in grain interiors,[14] is believed to be the cause for the extra strain hardening and hence high ductility in many gradient nanostructured materials.[13−16] Our results on diminished grain boundary softening process and extended partial dislocation slip, originating from the structure gradient, advance the fundamental understanding of the deformation mechanisms in gradient nanograined metals and shed light on the improved synergy of ductility and strength manifested in the emerging class of heterogeneous nanostructured materials.[9]

■ ASSOCIATED CONTENT

Supporting Information

The Supporting Information is available free of charge at https://pubs.acs.org/doi/10.1021/acs.nanolett.9b05202.

Details on molecular dynamics simulation, local shear strain, and defect analysis; additional data and figures including sample structures, grain size distribution, and grain boundary migration (PDF)

■ AUTHOR INFORMATION

Corresponding Author

Penghui Cao − *Department of Mechanical and Aerospace Engineering and Department of Materials Science and Engineering, University of California, Irvine, Irvine, California 92697, United States;* orcid.org/0000-0001-9866-5075; Email: caoph@uci.edu

Complete contact information is available at: https://pubs.acs.org/10.1021/acs.nanolett.9b05202

Notes

The author declares no competing financial interest.

■ ACKNOWLEDGMENTS

The author acknowledges the support from Department of Mechanical and Aerospace Engineering, UCI. The author would like to thank S. Yip (MIT), T.J. Rupert, and E.J. Lavernia (UCI) for helpful discussions, and the reviewers for providing helpful comments on the manuscript.

■ REFERENCES

(1) Hall, E. The deformation and ageing of mild steel: III discussion of results. *Proc. Phys. Soc., London, Sect. B* **1951**, *64*, 747.
(2) Petch, N. The cleavage strength of polycrystals. *J. Iron Steel Inst.* **1953**, *174*, 25−28.
(3) Zhu, T.; Li, J. Ultra-strength materials. *Prog. Mater. Sci.* **2010**, *55*, 710−757.
(4) Meyers, M. A.; Mishra, A.; Benson, D. J. Mechanical properties of nanocrystalline materials. *Prog. Mater. Sci.* **2006**, *51*, 427−556.
(5) Schiøtz, J.; Jacobsen, K. W. A maximum in the strength of nanocrystalline copper. *Science* **2003**, *301*, 1357−1359.
(6) Hahn, H.; Padmanabhan, K. A model for the deformation of nanocrystalline materials. *Philos. Mag. B* **1997**, *76*, 559−571.
(7) Nieh, T.; Wadsworth, J. Hall-Petch relation in nanocrystalline solids. *Scr. Metall. Mater.* **1991**, *25*, 955−958.
(8) Yip, S. The Strongest Size. (Nanocrystals). *Nature* **1998**, *391*, 532.
(9) Ma, E.; Zhu, T. Towards strength−ductility synergy through the design of heterogeneous nanostructures in metals. *Mater. Today* **2017**, *20*, 323−331.
(10) Wang, Y.; Chen, M.; Zhou, F.; Ma, E. High tensile ductility in a nanostructured metal. *Nature* **2002**, *419*, 912.
(11) Wu, X.; Zhu, Y. Heterogeneous materials: a new class of materials with unprecedented mechanical properties. *Mater. Res. Lett.* **2017**, *5*, 527−532.
(12) Wang, Y. M.; Voisin, T.; McKeown, J. T.; Ye, J.; Calta, N. P.; Li, Z.; Zeng, Z.; Zhang, Y.; Chen, W.; Roehling, T. T.; et al. Additively manufactured hierarchical stainless steels with high strength and ductility. *Nat. Mater.* **2018**, *17*, 63.
(13) Fang, T. H.; Li, W. L.; Tao, N. R.; Lu, K. Tensile Plasticity in Gradient Nano-Grained Copper. *Science* **2011**, *331*, 1587−1590.
(14) Cheng, Z.; Zhou, H.; Lu, Q.; Gao, H.; Lu, L. Extra strengthening and work hardening in gradient nanotwinned metals. *Science* **2018**, *362*, No. eaau1925.
(15) Wu, X.; Jiang, P.; Chen, L.; Yuan, F.; Zhu, Y. T. Extraordinary strain hardening by gradient structure. *Proc. Natl. Acad. Sci. U. S. A.* **2014**, *111*, 7197−7201.
(16) Wei, Y.; Li, Y.; Zhu, L.; Liu, Y.; Lei, X.; Wang, G.; Wu, Y.; Mi, Z.; Liu, J.; Wang, H.; et al. Evading the strength−ductility trade-off dilemma in steel through gradient hierarchical nanotwins. *Nat. Commun.* **2014**, *5*, 3580.
(17) Zeng, Z.; Li, X.; Xu, D.; Lu, L.; Gao, H.; Zhu, T. Gradient plasticity in gradient nano-grained metals. *Extreme Mechanics Letters* **2016**, *8*, 213−219.
(18) Schiotz, J.; Di Tolla, F.; Jacobsen, K. W. Softening of nanocrystalline metals at very small grain sizes. *Nature* **1998**, *391*, 561−563.
(19) Li, X.; Wei, Y.; Lu, L.; Lu, K.; Gao, H. Dislocation nucleation governed softening and maximum strength in nano-twinned metals. *Nature* **2010**, *464*, 877−880.
(20) Voronoi, G. Nouvelles applications des paramétres continus á théorie des formes quadratiques. Deuxième Mémoire. Recherches sur les parallélоèdres primitifs. *J. Reine Angew. Math.* **1909**, *1909*, 67.
(21) Foiles, S. M.; Baskes, M. I.; Daw, M. S. Embedded-atom-method functions for the fcc metals Cu, Ag, Au, Ni, Pd, Pt, and their alloys. *Phys. Rev. B: Condens. Matter Mater. Phys.* **1986**, *33*, 7983−7991.
(22) Nosé, S.; Nosī, S. Molecular Physics A molecular dynamics method for simulations in the canonical ensemble A molecular dynamics method for simulations in the canonical ensemblet. *Mol. Phys.* **1984**, *52*, 255−268.
(23) Hoover, W. G. Canonical dynamics: Equilibrium phase-space distributions. *Phys. Rev. A: At., Mol., Opt. Phys.* **1985**, *31*, 1695.
(24) Berendsen, H. J.; Postma, J. v.; van Gunsteren, W. F.; DiNola, A.; Haak, J. Molecular dynamics with coupling to an external bath. *J. Chem. Phys.* **1984**, *81*, 3684−3690.
(25) Shimizu, F.; Ogata, S.; Li, J. Theory of shear banding in metallic glasses and molecular dynamics calculations. *Mater. Trans.* **2007**, *48*, 2923.
(26) Wang, C.-C.; Mao, Y.-W.; Shan, Z.-W.; Dao, M.; Li, J.; Sun, J.; Ma, E.; Suresh, S. Real-time, high-resolution study of nanocrystalliza-

tion and fatigue cracking in a cyclically strained metallic glass. *Proc. Natl. Acad. Sci. U. S. A.* **2013**, *110*, 19725−19730.
(27) Cao, P.; Short, M. P.; Yip, S. Understanding the mechanisms of amorphous creep through molecular simulation. *Proc. Natl. Acad. Sci. U. S. A.* **2017**, *114*, 13631−13636.
(28) Cao, P.; Dahmen, K. A.; Kushima, A.; Wright, W. J.; Park, H. S.; Short, M. P.; Yip, S. Nanomechanics of slip avalanches in amorphous plasticity. *J. Mech. Phys. Solids* **2018**, *114*, 158−171.
(29) Rupert, T.; Gianola, D.; Gan, Y.; Hemker, K. Experimental observations of stressdriven grain boundary migration. *Science* **2009**, *326*, 1686−1690.
(30) Yamakov, V.; Wolf, D.; Phillpot, S. R.; Mukherjee, A. K.; Gleiter, H. Dislocation processes in the deformation of nanocrystalline aluminium by molecular-dynamics simulation. *Nat. Mater.* **2002**, *1*, 45.
(31) Rajabzadeh, A.; Mompiou, F.; Legros, M.; Combe, N. Elementary mechanisms of shear-coupled grain boundary migration. *Phys. Rev. Lett.* **2013**, *110*, 265507.
(32) Thomas, S. L.; Chen, K.; Han, J.; Purohit, P. K.; Srolovitz, D. J. Reconciling grain growth and shear-coupled grain boundary migration. *Nat. Commun.* **2017**, *8*, 1764.
(33) Jang, D.; Cai, C.; Greer, J. R. Influence of homogeneous interfaces on the strength of 500 nm diameter Cu nanopillars. *Nano Lett.* **2011**, *11*, 1743−1746.
(34) Shan, Z.; Stach, E.; Wiezorek, J.; Knapp, J.; Follstaedt, D.; Mao, S. Grain boundary-mediated plasticity in nanocrystalline nickel. *Science* **2004**, *305*, 654−657.
(35) Kumar, S.; Li, X.; Haque, A.; Gao, H. Is stress concentration relevant for nanocrystalline metals? *Nano Lett.* **2011**, *11*, 2510−2516.
(36) Hu, J.; Shi, Y.; Sauvage, X.; Sha, G.; Lu, K. Grain boundary stability governs hardening and softening in extremely fine nanograined metals. *Science* **2017**, *355*, 1292−1296.
(37) Khalajhedayati, A.; Pan, Z.; Rupert, T. J. Manipulating the interfacial structure of nanomaterials to achieve a unique combination of strength and ductility. *Nat. Commun.* **2016**, *7*, 10802.

https://dx.doi.org/10.1021/acs.nanolett.9b05202
Nano Lett. 2020, 20, 1440−1446